

Techno-economic Comparison of Thermochemical Energy Storage Systems Based on CaCO_3

C. Ortiz¹ [<https://orcid.org/0000-0002-7795-676X>], R. Chacartegui² [<https://orcid.org/0000-0001-7285-8661>], A. Carro² [<https://orcid.org/0000-0001-5841-8918>], S. García-Luna¹, J. Valverde^{2,3} [<https://orcid.org/0000-0002-8065-800X>], C. Tejada² and L. Pérez-Maqueda⁴ [<https://orcid.org/0000-0002-8267-3457>]

¹ Universidad Loyola Andalucía, Avenida de las Universidades s/n, 41704 Dos Hermanas, Spain

² Escuela Técnica Superior de Ingeniería, Universidad de Sevilla, Camino de los descubrimientos s/n, 41092 Sevilla, Spain

³ Virtualmechanics S.L, c/ Arquitectura 1, 41015 Sevilla, Spain

⁴ Instituto de Ciencia de Materiales de Sevilla (C.S.I.C.-Univ. Sevilla), Américo Vespucio 49, 41092 Sevilla, Spain

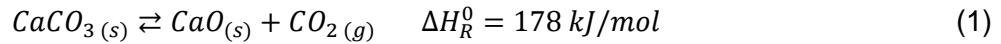
Abstract. Thermochemical Energy Storage (TCES) systems are a promising solution for integration into CSP plants. It allows to increase the overall efficiency and the capacity factor of the plant. Among the TCES; the CaCO_3/CaO process (the so-called CaL process) is the most studied system. Despite its low maturity, there is an increasing interest in the technology in the last few years, and the technology has been demonstrated at TRL5 (SOCRATCES H2020 project). This work evaluates the techno-economic performance of different CSP-CaL process integration. Several process schemes are modelled and evaluated in an hourly-basis simulation through the year. The results show that the LCOEs of the most profitable CaL-based systems are in the range of 147-208 €/MWh, allowing a capacity factor of up to 75%. Direct integration of the carbonator and a closed CO_2 Brayton cycle is the most profitable option. Designs with high-temperature solids storage are simpler (and cheaper) than those in which materials are stored at ambient temperature. The main challenges to improve plant reliability and reduce costs are increasing multicyclic CaO conversion and high-temperature cavity receiver efficiency.

Keywords: Energy storage, CSP, carbonates, Calcium-looping, Calcination

1. Introduction

Thermochemical energy storage (TCES) is an emerging concept with the potential to improve the capacity factor and overall efficiency of renewable power plants [1]. This technology has attracted great interest recently due to the potential advantages of its integration into CSP plants [1]. Concentrated solar energy is used to carry out the endothermic reaction of decomposition. The reaction products are stored separately, and when energy is required, they are mixed to release the stored energy through an exothermic reaction. To achieve an efficient and cost-effective thermochemical storage process, proper selection of the reversible reaction is a key issue. Among the recent proposals for thermochemical energy systems [2], those based on calcium carbonate are highly interesting [2]. The Calcium-Looping (CaL) process (Eq. 1) involves a theoretical energy storage density of around 3 GJ/m³ [3]. The energy stored can be released at temperatures above 800°C. These temperatures allow the

integration of very efficient power cycles. The process can be developed based on natural raw materials (limestone or dolomite), materials that are cheap (approx. 10€/ton), widely available, and environmentally friendly [4]. Recently, the technology has been successfully validated at TRL 5 within the H2020 SOCRATCES project [5]. In addition, the calcium-looping process is directly related to the well-known cement industry and has enormous potential as a CO₂ capture system (TRL 7), results that set the basis for potential further developments :



Recent works can be found in the literature with innovative CSP-CaL process schemes [4], including energy storage strategies at a wide range of temperatures, with the integration of different power cycles (combined cycle, regenerative CO₂ Brayton cycle, supercritical CO₂, Rankine, etc.), [6] and based on natural or synthetic materials [3]. However, there is a reduced number of economic analyses and projections. Moreover, they differ significantly from one work to another, especially those related to the capital costs of the different equipment in the process, making it difficult to objectively compare the potential integration schemes.

The present work develops a techno-economic comparison from several schemes recently proposed in the literature. Following a common methodology, these schemes are compared and discussed. All schemes are modelled and simulated using Typical Meteorological Year (TMY) data for the simulation (Seville, Spain) [7]. All this was taken from a global approach and a critical analysis of the current state of technology, with special attention to solar receiver integration, one of the main challenges of the CSP-CaL integration. The comparison includes process schemes in the net power range at the receiver from 5 MWth to 300 MWth.

2. Methodology

The methodology followed for developing the techno-economic comparison in this work is summarized in Figure 1. Different process flow diagrams recently published in the literature are evaluated. The technology behind these schemes, as well as potential new proposals, is analyzed based on the experience gained by the authors in the successful development of the SOCRATCES H2020 project.

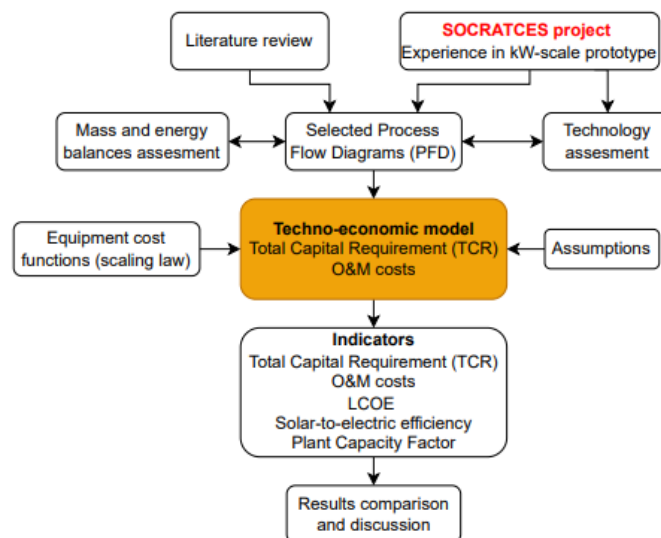


Figure 1. Methodology flowchart

The evaluation of mass and energy balances, as well as auxiliary calculations, is performed using Aspen Plus™ (CaL process modelling) and Thermoflex™ (power cycle). A preliminary solar field design is developed for each case using Solar Pilot [8]. A techno-economic analysis is developed from a quasi-stationary hourly model to compare the different process schemes based on relevant indicators.

3. Modelling

3.1. Solar field and receiver

The solar field for each scheme has been sized using Solar Pilot through a discrete Monte Carlo ray-tracing model (SolTrace [9]). A 360° heliostat solar field with up to 4 cavities (depending on the case of study) is considered in the design. The tower height also depends on the case, being 60 m (case 2; ~5 MWth net thermal power at the receiver) or 200 m for the rest of the cases. The cavities are evenly spaced, with one of them pointing straight to the geographical north. The layout of the heliostats has been optimized in SolarPilot following a radial stagger approach [8]. In the model, the heliostats have a reflectivity surface ratio of 97%, 95% mirror reflectivity, and a soiling factor of 95%. Atmospheric attenuation losses have been calculated according to DELSOL3 clear day model [8]. For the ray-tracing, a script has been generated that calculates the solar vector at different hours of the day using a NOAA simplified model [10]. The total incident power is calculated considering a 1000 W/m² solar direct normal irradiation (DNI). The incident power is then scaled to the actual DNI of the typical meteorological year data (TMY) in the simulation (Seville, Spain).

The receiver size is determined by the specific requirements in each study case. Each receiver is a flat panel composed of a bundle of vertical pipes and a diffuse reflective back surface so that the pipes are irradiated more homogeneously from all angles, front to back ratio. This assembly has not been modelled in this simulation and is simplified as a continuous flat surface. There is an important limitation to the design of the solar particle receiver. The residence time of the particles should be high enough to complete the calcination reaction. Calcination time has been widely evaluated within the SOCRATCES project [11]. The results show that around 60 seconds would be required under typical calcination conditions (pure CO₂ atmosphere, 950°C, 1 bar) to complete the reaction [12,13]. A 15-m-length cavity is considered, which involves a maximum particle velocity of around 0.3 m/s to guarantee an adequate residence time. The particles are moved to the top by pneumatic conveying, using CO₂ for fluidization. Particle velocity can be controlled with the CO₂ mass flow entering the receiver.

The receiver efficiency calculation is simplified by assuming a constant receiver efficiency as a function of the temperature (Eq. 2). Equation 2 assumes that the losses are basically due to radiation so that convective losses are neglected, which being a reasonably accurate approach for high temperatures, as in all proposed cases HTF temperatures are above 850°C. For simplicity in the analysis, the radiation view factor for the receiver with the environment is set with the value one (which is less accurate for cavities but on the conservative side). When comparing the different types of receiver proposed (air or particles), the heat transfer coefficients would be smaller in the case of air, which would increase the losses of this type of receiver compared to that of particles, which in general provides better heat transfer coefficients. More accurate receiver models must include CFD analysis to accurately assess thermal losses.

$$\eta_{receiver} = \frac{\alpha Q - \epsilon \sigma T^4}{Q} \quad (2)$$

Where T is the receiver temperature in K, α and ϵ are the absorptivity and emissivity of the receiver material (0.86 and 0.65, respectively, for Ni-based alloy tubes [14]), and it is assumed that Q is 600 kW/m² for all cases.

3.2. Proposed process flow diagrams

This section details the different cases evaluated. Five different Process Flow Diagrams (PFDs) are analyzed. Their main characteristics are shown in Table 1.

Table 1. Cases of study

PFD	Storage strategy	Power cycle	Solar receiver (net thermal power)	Reference
Case 1	Ambient temperature	Regenerative CO ₂ Brayton	Particle receiver (~100 MWth)	[4]
Case 2	Ambient temperature	Supercritical CO ₂	Particle receiver (~5 MWth)	[6,15]
Case 3	High-temperature	Vacuum CO ₂ Brayton	Particle receiver (~100 MWth)	[16]
Case 4	High-temperature	Regenerative CO ₂ Brayton	Volumetric gas receiver (~300 MWth)	[17]
Case 5	Ambient temperature	Supercritical CO ₂	Particle receiver (~100 MWth)	[6]

The first case is based on the work published by Chacartegui et al. [4], where the CaL TCEs concept was presented. The original process consists of a 100 MW-net particle receiver operating at 900°C. The CaCO₃ particles enter the receiver by pneumatic transport at high temperatures since the CaO particles preheat them, and the CO₂ leave separately from the receiver (after calcination occurs). After the heat recovery system of the calciner, the calcination products are stored at ambient temperature. A part of the stored material (1/3 under design conditions) is continuously fed to the carbonator, where the exothermic reactions release the stored heat for the production of electricity. The power cycle is based on a closed regenerative CO₂ Brayton cycle, where the CO₂ entering the carbonator at 3 bar (well above the stoichiometric amount that will be consumed in the reaction) is used as heat transfer fluid (HTF) between the reactor and the power cycle. Thus, CO₂ takes the heat released in carbonation and passes through the gas turbine, directly integrating the carbonator and the power block. In addition to the solar field and auxiliaries (pneumatic conveying system, cooling production, etc.), the whole process scheme accounts for the following equipment: solar particle receiver (working as calciner), 4 gas-solid heat exchangers, 1 gas-gas heat exchanger (regenerator), 1 solid-solid heat exchanger, 2 CO₂ compressors, 2 CO₂ turbines, 1 pressurized fluidized bed reactor, and 3 storage tanks (one of them for pressurized CO₂). More information on the process configuration and the assumption made can be found in [4]. The solar particle receiver is one of the critical equipments of the novel concept.

Case 2 (~5 MWth) and Case 5 (~100 MWth) are similar to the first, considering an indirect integration of a sCO₂ cycle for the power production of the heat released in the carbonator [6]. The efficiency of the turbomachine and pressure losses are taken from [15]. In this case, the CO₂ leaving the carbonator (operating at ambient pressure and 875°C) provides the heat

required for a supercritical carbon dioxide (sCO₂) recompression cycle. The differences in process equipment involved between these cases and Case 1 are: the main CO₂ turbine is removed, and two sCO₂ compressors and one sCO₂ turbine are added, two sCO₂ heat recuperators, a cooler and a CO₂-sCO₂ heat exchanger. Furthermore, the carbonator does not operate under pressure. Unlike Case 1, this integration of the CaL power cycle is not optimized from a thermal point of view, which reduces the efficiency of the process but also simplifies the system with a smaller number of heat exchangers and auxiliary equipment than more optimized systems [15,18].

Case 3 presents the novelty of storing the solids at high temperatures, which notably reduces the complexity of the heat recovery systems of the plant, as well as avoiding the use of solid-solid heat exchangers, but reducing the seasonal storage capacity. Hourly thermal losses are assumed to be 0.18% of the stored heat [19]. To improve the heat integration on the calciner side, a small-sized steam power cycle is integrated to produce the energy required for the compression of the CO₂ to be stored. Full information about this case is presented in [20,21]. The carbonator works at atmospheric pressure (850°C). CO₂ exiting the carbonator and used as HTF as in the previous case is expanded to 0.33 bar (PR=3) after a vacuum CO₂ Brayton cycle. The equipment required for this case is: solar particle receiver (working as calciner), 3 gas-solid heat exchangers, a small size steam power plant (HRSG, pump, cooler and steam turbine), 1 gas-gas heat exchanger (regenerator), 2 CO₂ compressors, 2 CO₂ turbines, 1 pressurized fluidized bed reactor, and 3 storage tanks (one of them for pressurized CO₂). More information on the process configuration and the assumptions made can be found in [4]. In addition to the solar particle receiver, the design and operation of the high-temperature lock hoppers at the solid storage tanks are critical. On the other hand, this configuration presents a reliable thermal integration of solids according to the current state-of-the-art technology [22].

Case 4 is based on the scheme proposed in [16]. This scheme presents key differences with respect to the previous cases. A pressurized receiver (which could be a tube-based system or a volumetric system) [23] is considered instead of a particle receiver, in which air is used as HTF. The hot air exiting the receiver (850°C) passes through a heat exchanger coupled to the calciner, providing, indirectly, the required heat for the calcination. After the reactor, the HTF continues to complete a typical path of a regenerative CO₂ Brayton cycle. This scheme presents the advantage of avoiding the use of a particle receiver, which is the most critical component for the integration of CSP-CaL [22]. Another key aspect is that in this scheme, calcination occurs under partial pressure, which allows the calcination temperature to be reduced below 900°C. Concretely, this case proposes to carry out the calcination at 0.01 bar. The laboratory test demonstrated that a temperature of 765°C is sufficient to complete the reaction in a short residence time [24]. Low-pressure calcination enhances CaO conversion (represented as X) due to the reduction in particle sintering, which highly penalizes the maximum carbonation conversion [25]. Thus, a residual CaO conversion of X=0.42 is demonstrated at the laboratory scale [24] instead of a CaO conversion of X=0.15 under typical calcination conditions (900-950°C, 1 bar) [3]. Another difference from the previous schemes is to consider the use of fine particles (average size 45 µm instead of 200-300 µm as typical in fluidized bed reactors), which allows the use of an inclined flow reactor and promotes the kinetics of the reaction due to the lower sizes of the particles [26]. In this case, a single reactor is considered, working as either calciner or carbonator. When stored energy is required, air continues to enter the power cycle, being heated before the gas turbine by the heat release in the carbonator.

The different PFDs are modelled from the process scheme and the assumptions indicated in

each reference work. A quasi-stationary hourly analysis is carried out by combining Excel and the different software used in the reference works, namely, EES¹ (case 1, case 2, case 5), Aspen Plus² (case 3), and Thermoflex³ + Aspen Plus (case 4).

3.3. Economic framework

The techno-economic model is based on the analysis of capital requirements (CAPEX) and operating and maintenance costs (OPEX). The proposed model for calculating the total capital requirement (TCR) is based on [10]. The core of a cost estimate is the Bare Erected Cost (BEC), which is quantified on the basis of an itemized list of all process equipment required for a project, together with the estimated cost of all materials and labour needed to complete the installation. The cost of additional support facilities needed for the project is estimated as a percentage of the process costs to produce the BEC.

Table 2. Capital cost estimates

Process equipment	Engineering-economic method [27]
Piping	10% [28]
Electrical	5% [28]
Instrumentation and control	5% [28]
Materials	7% [28]
Labor (direct & indirect)	18% [29]
Bare Erected Cost (BEC)	
Engineering services (EPC)	5% [30]
Process contingencies	20% [30]
Project contingencies	20% (preliminary) [30]
Total Plant Cost (TPC)	
Owner's costs	7% [28]
Total Overnight Cost (TOC)	
Interest during construction (IDC)	Not considered
Total Capital Requirement (TCR)	

The purchase cost of equipment is estimated from correlations based on key scaling parameters. Further information about the correlations used can be found as follows: air and CO₂ turbomachinery [31,32], sCO₂ turbomachinery [33], solar side components (particle receiver, tower, and heliostats) [34], gas-solid heat exchangers [18], gas-gas heat exchanger coolers and cooling tower [32], cyclones [35], steam cycle and heat recovery system [36] and storage vessels [37]. All costs are updated to 2021 as a reference cost year using the CEPCI index. The solid-solid heat exchanger is calculated as two interconnected gas-solid heat exchangers, increasing their cost by 50% due to the low maturity of this equipment. The same procedure is followed for the solid particle receiver that works as a calciner, whose costs are increased by 100% due to the lack of experimental results on a large scale. Additional fees for engineering services are generally estimated as a percentage of the BEC

¹ <https://www.fchartsoftware.com/ees/>

² <https://www.aspentech.com/>

³ <https://www.thermoflow.com/>

[30]. Due to their lower maturity level, process contingencies are assumed to be 20%. Table 2 summarizes the procedure for estimating total capital costs. Regarding operational costs (OPEX), fixed and variable costs are estimated as 66 \$/kW and 3.5 \$/MWh respectively [38].

The following indicators have been selected to evaluate and compare the performance of the proposed systems:

- Levelized Cost of Energy (LCOE): It represents the cost of electricity generation (in €/MWh) over the life of the power plant [30]. For its calculation (Eq. 3), in this work is assumed the methodology proposed in [38,39]. This method is appropriate for preliminary stages of project feasibility analysis.

$$LCOE = \frac{FCR \cdot TCR + FOC}{AEP} + VOC \quad (3)$$

where TCR is the total capital requirement (€), FOC is the total fixed O&M costs (€), VOC is the total variable O&M costs (€/kWh), AEP is the annual electricity production (kWh). FCR is the fixed charge rate, the annual return as a fraction of the capital cost, which is calculated according to Eq. 4:

$$FCR = CRF \cdot PFF \cdot CFF \quad (4)$$

where, PFF is the project financing factor, CFF is the construction financing factor, and CRF is the capital recovery factor, which is calculated according to [38]. By considering a period of 25 years, 2.5%/year inflation rate, 13%/year internal rate of return and 4%/year nominal debt interest rate, FCR results in 0.0719.

- Capacity Factor: it represents the energy produced in a year divided by the product of nominal capacity of the plant multiplied by the number of hours in a year [40].

4. Results

In this work, three different solar field designs are considered, depending on the case. Design 1, applied to Case 1, Case 3 and Case 5, is based on a particle solar receiver (~100 MW_{th} net) with four cavities evenly spaced at 90°. Design 2 involves a notably smaller solar field, with only one cavity and a ~5 MW_{th} net particle receiver. Design 3 consists of a pressurized air cavity receiver (~100 MW_{th}) with a 360-degree heliostat solar field with three cavity receivers on top. Table 3 shows the main inputs for the solar field designs as well as the performance obtained. Receiver efficiency is calculated as indicated in Section 3.1. The flux density at the receivers is in the same order as that of current commercial or tested systems (i.e. SOLUGAS [41]); therefore, they are evaluated as technically feasible. Due to the high temperature required at the receiver (~900°C), SiC-based materials could be required for the receiver pipes.

Once the different solar fields are designed, the process schemes (Section 3.2) are simulated on an hourly basis throughout the year. The schemes have different energy storage strategies originally proposed in their respective publications. Figure 2 represents the sum of the ratio of the total power production in each hour to the maximum power production according to Equation 4. Therefore, Figure 2 illustrates the daily pattern followed throughout the year.

$$R = \sum \frac{\text{power production in the } i\text{-hour}}{\text{maximum power production}} \quad (4)$$

Table 3. Solar field design and results on the 21st of June in Seville

	Solar field designs		
	Design 1	Design 2	Design 3
	Case 1; Case 3 and Case 5	Case 2	Case 4
Design DNI (W/m ²)	950	950	950
Receiver temperature (°C)	900	900	850
Number of cavities	4	1	3
Cavity aperture, H x W (m)	15 x 15	13 x 3	8.4 x 12
Tower height (m)	200	60	200
Simulated heliostat area (m ²)	209485	11702	531343
Simulated heliostat count	5999	754	3804
Power incident on field (KW)	188537	11117	478209
Power absorbed by the receiver (kW)	145533	7689.9	283013
Power absorbed by HTF (kW)	108233	5719	215741
Cloudiness efficiency (%)	100	100	100
Shadowing and Cosine efficiency (%)	88.28	88.71	83.2
Reflection efficiency (%)	87.59	90.25	90
Blocking efficiency (%)	99.9	99.34	97.6
Image intercept efficiency (%)	99.93	88.88	80.9
Solar field optical efficiency (%)	77.19	69.17	59.2
Optical efficiency incl. receiver (%)	57.40	51.44	40.00

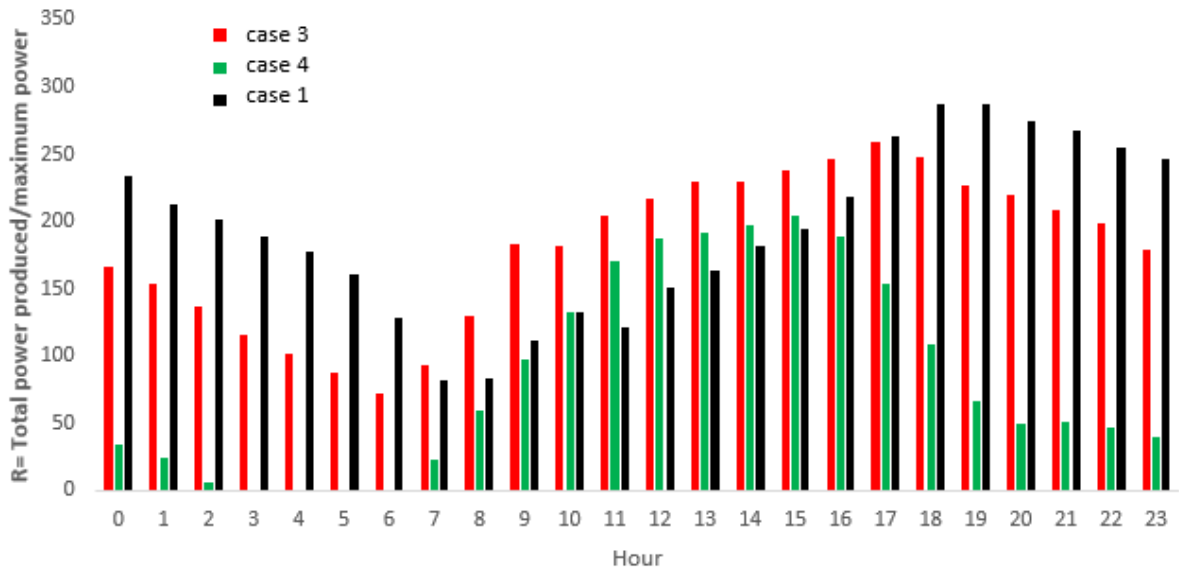


Figure 2. Comparison of the power production along the day for several cases

As can be seen, Case 1 and Case 3 present a notably higher energy storage capacity than Case 4, which is built on their different Solar Multiples (SM): 3, 2.7 and 1.3, respectively. By comparing case 1 and case 3 (~100 MW_{th} net particle receiver), the designs involve greater power production that occurs in the former from 5 pm to 6 am. The design nominal capacities are 14.03 and 11.86 MWe, respectively. However, power production in case 1 is penalized

during 'day' hours (7 am-4 pm) due to higher energy consumption for CO₂ compression. In case 1 strategy [4], all CO₂ produced in the calciner is compressed and stored (75 bar), whereas in case 3 [20] a certain amount of CO₂ (SM=2.7) is compressed and stored while the rest is sent directly to carbonation (which operates at atmospheric pressure) for power production, which involves a reduction in power consumption associated to hours with higher solar irradiance. Case 4 presents a lower energy storage potential, with a notably small power production after sunset. This represents a soft integration of the novel TCES system, increasing the reliability of the system with current state-of-the-art technology and thus reducing potential risks [16].

Table 4 shows the yearly results and the techno-economic performance of each case. For comparison purposes, the solar field designed according to Section 3.1 (Design 1) is simulated within a typical molten salt-based tower plant. Two tanks of molten salts with a 16 h full load hours of storage are considered. The design power cycle net output is assumed to be 14 MWe (41.2% cycle thermal efficiency), in the same order as in Case 1 and Case 3. CAPEX and OPEX are assumed according to [42], while the same financial parameters are assumed as in CaL-based cases (Section 3.3). The model is simulated using SAM [38] from the same climatic data as in the rest of the cases. The LCOE and the capacity factor obtained are within the expected according to the state-of-the-art technology [43].

Table 4. Results and techno-economic performance

	Ref.	Case 1	Case 2	Case 3	Case 4	Case 5
Solar field	Design 1	Design 1	Design 2	Design 1	Design 3	Design 1
Average CaO conversion	-	0.15	0.15	0.15	0.42	0.15
Solar Multiple	3	3	3	2.7	1.3	3
Design nominal capacity (MWe)	14.00	14.03	0.51	11.86	91.00	8.48
CaO maximum storage capacity (m3)	-	3908	201	3062	753	3936
solids maximum storage capacity (m3)	-	2672	134	2097	615	2672
CO ₂ maximum storage capacity (m3)	-	473	32	462	322	579
Yearly energy production (GWh)	68.19	72.06	3.36	76.46	183.91	57.39
Yearly efficiency (receiver to electric)	35.94%	35.40%	27.14%	37.56%	39.17%	28.19%
Yearly efficiency (solar to electric)	14.63%	15.47%	12.52%	16.41%	15.56%	12.32%
Capacity factor	55.6%	59%	75%	74%	23%	77%
Bare Erected Cost (M€)	-	119.94	16.71	127.06	229.91	157.31
EPC cost	-	125.34	17.47	132.77	240.25	164.39
TPC	-	175.48	24.45	185.88	336.35	230.15
TCR	165.61	192.91	24.24	198.91	273.00	240.24
LCOE (€/MWh)	200.70	208.20	551.60	201.60	147.00	314.20

Case 1 and case 3, with the same solar field design, present a similar value of LCOE, with a notably higher capacity factor in case 3. In those cases, the higher total capital requirement (TCR) is compensated with higher yearly efficiency. Comparing cases 1, 3 and 5 (all of them with the same solar side design) shows that the direct integration of the carbonator-power cycle (case 1 and 3) is more profitable than the indirect integration. In addition, the high costs considered for sCO₂ turbomachinery and heat exchangers causes a higher cost of the system. The CaL-based systems present the peculiarity that the net energy production during the daytime hours is notably different from the production during the night hours, due to the large energy consumption made for the compression of the CO₂ to be stored during the daytime hours. The lower energy penalty due to compression in case 3 (because part is sent

directly to the carbonator) allows a greater energy production with respect to case 1, which, together with a simpler energy integration, results in a lower LCOE.

Case 4 is the cheapest, mainly due to the larger size of the system and a lower capacity factor since the storage system (and its associated subsystems) are smaller in this case. Another important factor in case 4 is that the conversion of CaO is much higher, which implies a lower need for storage, heating, transportation, etc., of inert solids throughout the plant. This implies better energy efficiency and smaller size of the equipment. Thus, the higher the CaO conversion the higher energy storage density, which involves a lower storage volume to produce the same amount of power. As showed in [20], for CaO conversion around $X=0.15$, energy storage density is similar to molten-salts based plants. As expected, case 2 is the more expensive case due to the high cost associated with the power cycle and the lower efficiency in the indirect integration of the carbonation and power cycle in comparison with the direct integration and the economy of scale.

5. Conclusions

Thermochemical energy storage systems based on CaCO₃ have the potential to improve solar-to-electric efficiency and increase the capacity factor of CSP plants. Among the CSP-CaL processes evaluated, the most profitable cases provide a LCOE in the range of 147-208 €/MWh, allowing a capacity factor of up to 75%. Moreover, the system significantly reduces water consumption and the storage materials are abundant worldwide and environmentally friendly. Direct integration of the carbonator and a closed CO₂ Brayton cycle is the most profitable option, and designs with high-temperature solids storage are the simplest cases from an energy integration perspective. However, there are key challenges to solve to increase both the reliability and the profitability of these systems. First, it is fundamental to increase CaO conversion above the typical value ($X=0.15$). This can be achieved by reducing the calcination pressure (as in Case 4) or by varying other process design conditions (make-up flow of fresh material, reaction temperature, etc.). In addition, it is key to gain experimental knowledge and optimize the design of high-temperature receivers to reduce the thermal losses.

Author contributions

C. Ortiz: Conceptualization, Methodology, Modelling and simulations, Writing-Original draft preparation; R. Chacartegui: Reviewing and Editing, Funding Acquisition; A. Carro: Investigation; S. Garcia: Investigation; J. Valverde: Methodology, Modelling; C. Tejada: Methodology, Modelling and simulations; Luis A. Pérez-Maqueda: Reviewing and Editing, Funding Acquisition.

Acknowledgement

The research leading to these results has received funding from the Junta de Andalucía (grant number PY20 RE007) and the Spanish Government (grant number PDC2021-121552-C21).

References

- [1] International Renewable Energy Agency. Innovation Outlook: Thermal Energy Storage. 2020.
- [2] Carrillo AJ, González-Aguilar J, Romero M, Coronado JM. Solar Energy on Demand: A Review on High Temperature Thermochemical Heat Storage Systems and

Materials. Chem Rev 2019;119:4777–816.
<https://doi.org/10.1021/acs.chemrev.8b00315>.

- [3] Ortiz C, Valverde JM, Chacartegui R, Perez-Maqueda LA, Giménez P. The Calcium-Looping (CaCO₃/CaO) process for thermochemical energy storage in Concentrating Solar Power plants. *Renew Sustain Energy Rev* 2019;113:109252. <https://doi.org/10.1016/j.rser.2019.109252>.
- [4] Chacartegui R, Alovio A, Ortiz C, Valverde JMM, Verda V, Becerra JAA. Thermochemical energy storage of concentrated solar power by integration of the calcium looping process and a CO₂ power cycle. *Appl Energy* 2016;173:589–605.
- [5] SOLar Calcium-looping integRation for Thermo-Chemical Energy Storage | SOCRATCES Project | H2020 | CORDIS | European Commission n.d.
- [6] Ortiz C, Chacartegui R, Valverde JMM, Alovio A, Becerra JAA. Power cycles integration in concentrated solar power plants with energy storage based on calcium looping. *Energy Convers Manag* 2017;149:815–29. <https://doi.org/10.1016/j.enconman.2017.03.029>.
- [7] European Comission. Photovoltaic geographical information system (PVGIS) n.d.
- [8] Turchi CS, Boyd M, Kesseli D, Kurup P, Mehos M, Neises T, et al. CSP Systems Analysis - Final Project. Nrel/Tp-5500-72856 2019.
- [9] Ho CK. Software and Codes for Analysis of Concentrating Solar Power Technologies. 2008.
- [10] National Renewable energy laboratory (NREL). SolarPILOT (Solar Power tower Integrated Layout and Optimization Tool) n.d.
- [11] Socratces Project, 2018 n.d.
- [12] Lisbona P, Bailera M, Hills T, Sceats M, Díez LI, Romeo LM. Energy consumption minimization for a solar lime calciner operating in a concentrated solar power plant for thermal energy storage. *Renew Energy* 2020;156:1019–27. <https://doi.org/10.1016/j.renene.2020.04.129>.
- [13] Ortiz C, Valverde J, Tejada C, Carro A, Chacartegui R, Valverde JM, et al. Solar-driven indirect calcination for thermochemical energy storage. *SolarPACES Int. Conf.*, vol. 160012, 2022, p. 160012. <https://doi.org/10.1063/5.0085705>.
- [14] Balat-Pichelin M, Sans JL, Bêche E, Charpentier L, Ferrière A, Chomette S. Emissivity at high temperature of Ni-based superalloys for the design of solar receivers for future tower power plants. *Sol Energy Mater Sol Cells* 2021;227. <https://doi.org/10.1016/j.solmat.2021.111066>.
- [15] Tesio U, Guelpa E, Verda V. Integration of ThermoChemical Energy Storage in Concentrated Solar Power. Part 2: comprehensive optimization of supercritical CO₂ power block. *Energy Convers Manag X* 2020;6:100038. <https://doi.org/10.1016/j.ecmx.2020.100038>.
- [16] Ortiz C, Carro A, Chacartegui R, Valverde JM, Perejón A, Sánchez-Jiménez PE, et al. Low-pressure calcination to enhance the calcium looping process for thermochemical energy storage. *J Clean Prod* 2022;363:132295. <https://doi.org/10.1016/J.JCLEPRO.2022.132295>.

- [17] Ortiz C, Carro A, Chacartegui R, Valverde JM, Perejón A, Sánchez-Jiménez PE, et al. Low-pressure calcination to enhance the calcium looping process for thermochemical energy storage. *J Clean Prod* 2022;363:132295. <https://doi.org/10.1016/j.jclepro.2022.132295>.
- [18] Tesio U, Guelpa E, Verda V. Integration of thermochemical energy storage in concentrated solar power. Part 1: Energy and economic analysis/optimization. *Energy Convers Manag X* 2020;6:100039. <https://doi.org/10.1016/j.ecmx.2020.100039>.
- [19] Peng X, Yao M, Root TW, Maravelias CT. Design and Analysis of Concentrating Solar Power Plants with Fixed-bed Reactors for Thermochemical Energy Storage. *Appl Energy* 2020;262:114543. <https://doi.org/10.1016/j.apenergy.2020.114543>.
- [20] Ortiz C, Romano MC, Valverde JM, Binotti M, Chacartegui R. Process integration of Calcium-Looping thermochemical energy storage system in concentrating solar power plants. *Energy* 2018;155:535–51. <https://doi.org/10.1016/j.energy.2018.04.180>.
- [21] Ortiz C, Binotti M, Romano MC, Valverde JM, Chacartegui R. Off-design model of concentrating solar power plant with thermochemical energy storage based on calcium-looping. *AIP Conf. Proc.*, vol. 210006, 2019, p. 210006. <https://doi.org/10.1063/1.5117755>.
- [22] Ortiz C, Valverde JM, Chacartegui R, Pérez-Maqueda LA, Gimenez-Gavarrell P. Scaling-up the Calcium-Looping Process for CO₂ Capture and Energy Storage. *KONA Powder Part J* 2021;38:189–208. <https://doi.org/10.14356/kona.2021005>.
- [23] Stein WH, Buck R. Advanced power cycles for concentrated solar power. *Sol Energy* 2017;152:91–105. <https://doi.org/10.1016/j.solener.2017.04.054>.
- [24] Sarrión B, Perejón A, Sánchez-Jiménez PE, Amghar N, Chacartegui R, Manuel Valverde J, et al. Calcination under low CO₂ pressure enhances the calcium Looping performance of limestone for thermochemical energy storage. *Chem Eng J* 2020;127922. <https://doi.org/10.1016/j.cej.2020.127922>.
- [25] Benitez-Guerrero M, Valverde JM, Sanchez-Jimenez PE, Perejon A, Perez-Maqueda LA. Multicycle activity of natural CaCO₃ minerals for thermochemical energy storage in Concentrated Solar Power plants. *Sol Energy* 2017;153:188–99. <https://doi.org/10.1016/j.solener.2017.05.068>.
- [26] Scaltsoyiannes A, Lemonidou A. CaCO₃ decomposition for calcium-looping applications: Kinetic modeling in a fixed-bed reactor. *Chem Eng Sci X* 2020;8:100071. <https://doi.org/10.1016/j.cesx.2020.100071>.
- [27] IEAGHG. IEAGHG Technical Review Towards improved guidelines for cost evaluation of carbon capture and storage 2021-TR05 2021.
- [28] De Lena E, Spinelli M, Gatti M, Scaccabarozzi R, Campanari S, Consonni S, et al. Techno-economic analysis of calcium looping processes for low CO₂ emission cement plants. *Int J Greenh Gas Control* 2019:244–60. <https://doi.org/10.1016/j.ijggc.2019.01.005>.
- [29] Turton R, Bailie RC, Whiting WB, Shaeiwitz JA, Bhattacharyya D. Analysis, Synthesis, and Design of Chemical Processes. vol. 40. 2001. [https://doi.org/10.1002/1521-3773\(20010316\)40:6<9823::AID-ANIE9823>3.3.CO;2-C](https://doi.org/10.1002/1521-3773(20010316)40:6<9823::AID-ANIE9823>3.3.CO;2-C).
- [30] IEAGHG. Toward a Common Method of Cost Estimation for CO₂ Capture and Storage At Fossil Fuel Power Plants 2013.

- [31] Benjelloun M, Douleris G, Singh R. A method for techno-economic analysis of supercritical carbon dioxide cycles for new generation nuclear power plants. *Proc Inst Mech Eng Part A J Power Energy* 2012;226:372–83. <https://doi.org/10.1177/0957650911429643>.
- [32] Michalski S, Hanak DP, Manovic V. Techno-economic feasibility assessment of calcium looping combustion using commercial technology appraisal tools. *J Clean Prod* 2019;219:540–51. <https://doi.org/10.1016/j.jclepro.2019.02.049>.
- [33] Carlson MD, Middleton BM, Ho CK. Techno-economic comparison of solar-driven SCO₂ brayton cycles using component cost models baselined with vendor data and estimates. *ASME 2017 11th Int Conf Energy Sustain ES 2017, Collocated with ASME 2017 Power Conf Jt with ICOPE 2017, ASME 2017 15th Int Conf Fuel Cell Sci Eng Technol ASME 2017*:1–7. <https://doi.org/10.1115/ES2017-3590>.
- [34] Ho CK. A review of high-temperature particle receivers for concentrating solar power. *Appl Therm Eng* 2016;109:958–69. <https://doi.org/10.1016/j.applthermaleng.2016.04.103>.
- [35] De Lena E, Spinelli M, Gatti M, Scaccabarozzi R, Campanari S, Consonni S, et al. Techno-economic analysis of calcium looping processes for low CO₂ emission cement plants. *Int J Greenh Gas Control* 2019;82:244–60. <https://doi.org/10.1016/j.ijggc.2019.01.005>.
- [36] Haaf M, Anantharaman R, Roussanaly S, Ströhle J, Eppe B. CO₂ capture from waste-to-energy plants: Techno-economic assessment of novel integration concepts of calcium looping technology. *Resour Conserv Recycl* 2020;162:104973. <https://doi.org/10.1016/j.resconrec.2020.104973>.
- [37] Bayon A, Bader R, Jafarian M, Fedunik-Hofman L, Sun Y, Hinkley J, et al. Techno-economic assessment of solid–gas thermochemical energy storage systems for solar thermal power applications. *Energy* 2018;149:473–84. <https://doi.org/10.1016/j.energy.2017.11.084>.
- [38] National Renewable Energy Laboratory. Golden C. System Advisor Model Version 2017.1.17 (SAM 2017.1.17) n.d.
- [39] Short W, Packey D, Holt T. A manual for the economic evaluation of energy efficiency and renewable energy technologies. *Renew Energy* 1995;95:73–81. <https://doi.org/NREL/TP-462-5173>.
- [40] International Renewable Energy Agency (IRENA). Concentrating Solar Power. Renewable energy technologies: cost analysis series. vol. 1. 2012. <https://doi.org/10.1016/B978-0-12-812959-3.00012-5>.
- [41] Quero M, Korzynietz R, Ebert M, Jiménez AA, del Río A, Brioso JA. Solugas – Operation Experience of the First Solar Hybrid Gas Turbine System at MW Scale. *Energy Procedia* 2014;49:1820–30. <https://doi.org/10.1016/j.egypro.2014.03.193>.
- [42] Turchi CS, Heath GA. Molten Salt Power Tower Cost Model for the System Advisor Model (SAM). Technical Report: NREL/TP-5500-57625. Natl Renew Energy Lab USA 2013;5500–57625:1–53.
- [43] International Renewable Energy Agency. Renewable Power Generation Costs in 2021. 2021.